

Physics and Technology

Emitters

Materials

Infrared emitting diodes (IREDs) can be produced from a range of different III-V compounds. Unlike the elemental semiconductor silicon, the compound III-V semiconductors consists of two or more different elements of group three (e.g., Al, Ga, In) and five (e.g., P, As) of periodic table. Bandgap energies of these compounds vary between 0.18 eV and 3.4 eV. However, IREDs considered here emit in the near infrared spectral range between 800 nm and 1000 nm, and, therefore, selection of materials is limited to GaAs and mixed crystal $\text{Ga}_{1-x}\text{Al}_x\text{As}$, $0 \leq x \leq 0.8$, made from pure compounds GaAs and AlAs.

Infrared radiation is produced by radiative recombination of electrons and holes from the conduction and valence bands. Emitted photon energy, therefore, corresponds closely to bandgap energy E_g . Emission wavelength can be calculated according to the formula $\lambda(\mu\text{m}) = 1.240 / E_g(\text{eV})$. Internal efficiency depends on band structure, doping material and doping level. Direct bandgap materials offer high efficiencies, because no phonons are needed for recombination of electrons and holes. GaAs is a direct gap material and $\text{Ga}_{1-x}\text{Al}_x\text{As}$ is direct up to $x = 0.44$. Doping species Si provides best efficiencies and shifts emission wavelength below bandgap energy into infrared spectral range by about 50 nm typically. Charge carriers are injected into material via pn junctions. Junctions of high injection efficiency are readily formed in GaAs and $\text{Ga}_{1-x}\text{Al}_x\text{As}$. P-type conductivity can be obtained with metals of valency two, such as Zn and Mg, n-type conductivity with elements of valency six, such as S, Se and Te. However, silicon of valency four can occupy sites of III-valence and V-valence atoms, and, therefore, acts as donor and as acceptor. Conductivity type depends primarily on material growth temperature. By employing exact temperature control, pn junctions can be grown with the same doping species Si on both sides of the junction. Ge, on the other hand, also has a valency of four, but occupies group V sites at high temperatures i.e., p-type.

Only mono crystalline material is used for IRED production. In the mixed crystal system $\text{Ga}_{1-x}\text{Al}_x\text{As}$, $0 \leq x \leq 0.8$, lattice constant varies only by about 1.5×10^{-3} . Therefore, mono crystalline layered structures of different $\text{Ga}_{1-x}\text{Al}_x\text{As}$ compositions can be produced with extremely high structural quality. These structures are useful because bandgap can be

shifted from 1.40 eV (GaAs) to values beyond 2.1 eV which enables transparent windows and heterogeneous structures to be fabricated. Transparent windows are another suitable means to increase efficiency, and heterogeneous structures can provide shorter switching times and higher efficiency. Such structures are termed single hetero (SH) or double hetero structures (DH). DH consist normally of two layers that confine a layer with a much smaller bandgap.

Best production method for all materials needed is liquid phase epitaxy (LPE). This method uses Ga-solutions containing As, possibly Al, and doping substance. The solution is saturated at high temperature, typically 900 °C, and GaAs substrates are dipped into liquid. The solubility of As and Al decreases with decreasing temperature. In this way epitaxial layers can be grown by slow cooling of the solution. Several layers differing in composition may be obtained using different solutions one after another, as needed e.g. for DHs.

In liquid phase epitaxial reactors, production quantities of up to 50 wafers, depending on type of structure required, can be handled.

IRED Chips and Characteristics

At present, the most popular IRED chip is made only from GaAs. Structure of the chip is displayed in figure 1.

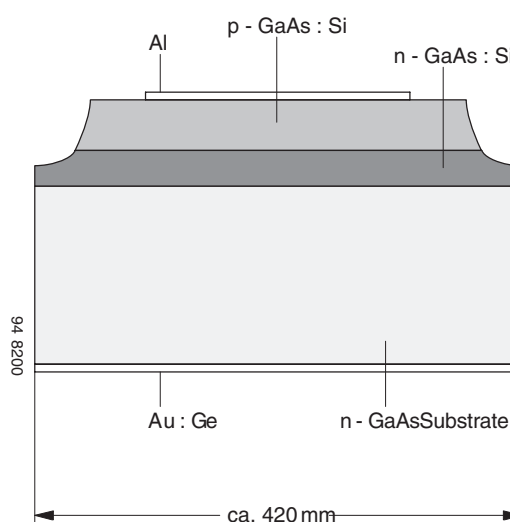


Figure 1.

On an n-type substrate, two Si-doped layers are grown by liquid phase epitaxy from the same solution

producing an emission wavelength of 950 nm. Growth starts as n-type at high temperature and becomes p-type below about 820 °C. A structured Al-contact on p-side and a large area Au:Ge contact on back side provide a very low series resistance.

The angular distribution of emitted radiation is displayed in figure 2.

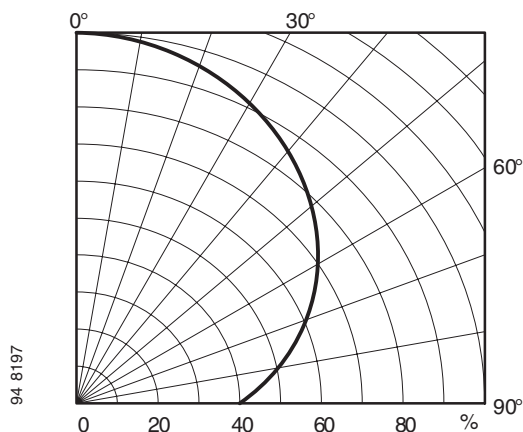


Figure 2.

Package of the chip has to provide good collection efficiency of radiation emitted sideways, and has to diminish refractive index step between chip ($n = 3.6$) and the air ($n = 1.0$) with an epoxy of refractive index 1.55. In this way, output power of chip is increased by a factor of 3.5 for the assembled device.

The chip described is the most cost-efficient one. Forward voltage at $I_F = 1.5$ A has lowest possible value. Total series resistance is typically only 0.60Ω . Output power and linearity (defined as optical output power increase, divided by current increase between 0.1 and 1.5 A) are high. Relevant data on chip and a typical assembled device are given in table 1.

Technology used for a chip emitting at 880 nm eliminates absorbing substrate and uses only a thick epitaxial layer. Chip is shown in figure 3.

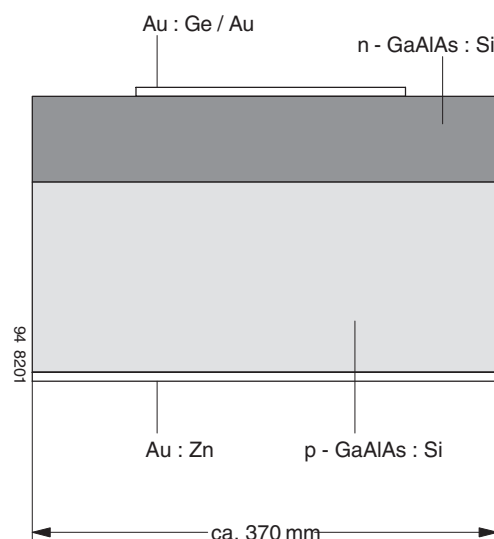


Figure 3.

Originally, the GaAs substrate was adjacent to the n-side. Growth of $\text{Ga}_{0.7}\text{Al}_{0.3}\text{As}$ started as n-type and became p-type – as in the first case – through the specific properties of doping material Si. A characteristic feature of Ga-Al-As phase system causes Al-content of growing epitaxial layer to decrease. This causes Al-concentration at the junction to drop to 8 % ($\text{Ga}_{0.92}\text{Al}_{0.08}\text{As}$), producing an emission wavelength of 880 nm. During further growth the Al-content approaches zero. Gradient of the Al-content and correlated gradient of bandgap energy, produces an emission band of a relatively large half width. Transparency of the large bandgap material results in a high external efficiency on this type of chip.

Chip is mounted n-side up, and front side metallization is Au:Ge/Au, whereas reverse side metallization is Au:Zn.

Angular distribution of the emitted radiation is displayed in figure 4.

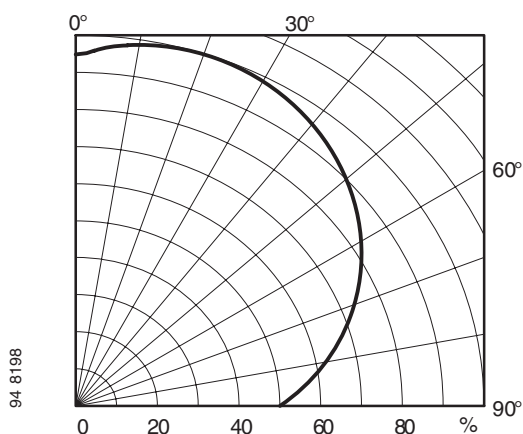


Figure 4.

Due to its shorter wavelength, $\text{Ga}_{1-x}\text{Al}_x\text{As}$ chip described offers specific advantages in combination with a Si detector. Integrated Opto-ICs, like amplifiers or Schmitt Triggers, have higher sensitivities at shorter wavelengths. Similarly, phototransistors are also more sensitive. Finally, frequency bandwidth of pin diodes is higher at shorter wavelengths. This chip also has the advantage of having high linearity up to and beyond 1.5 A. Forward voltage, however, is higher than voltage of a GaAs chip. Table 2 (see „Symbols and Terminology“) provides more data on the chip.

A technology combining some of the advantages of the two technologies described above is summarized in figure 5.

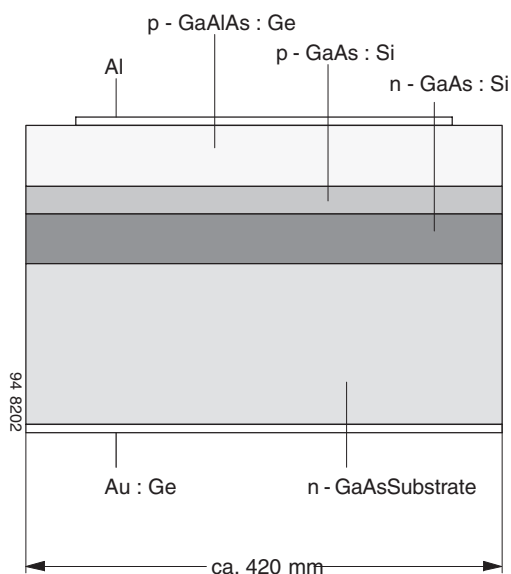


Figure 5.

Starting with n-type substrate, n- and p-type GaAs layers are grown in a similar way to epitaxy of standard GaAs:Si diode. After this, a highly transparent window layer of $\text{Ga}_{1-x}\text{Al}_x\text{As}$, doped p-type is grown. The upper contact to p-side is made of Al and the rear side contact is Au:Ge. Angular distribution of emitted radiation is shown in figure 6.

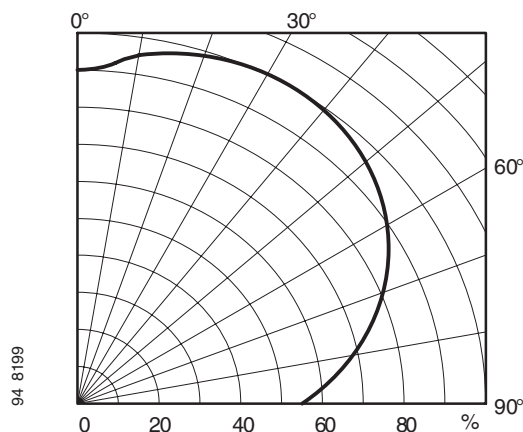


Figure 6.

This chip type combines a relatively low forward voltage with a high electro-optical efficiency, offering optimized combination between the advantageous characteristics of the two other chips. Refer again to table 2 (see „Symbols and Terminology“) for more details.

As mentioned in previous section, double heterostructures (DH) provide even higher efficiencies and

faster switching times. A schematic representation of such a chip is shown in figure 7.

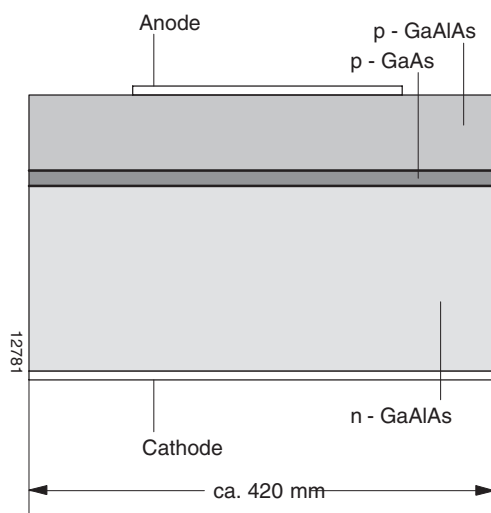


Figure 7.

Active layer is depicted as the thin layer between p- and n- type $\text{Ga}_{1-x}\text{Al}_x\text{As}$ confinement layers.

Contacts are dependent on polarity of the chip. If p is up, then p-side contact is Al, the back side Au:Ge, and if n is up, then this side has a Au:Ge contact and back side Au:Zn. Two such chips that are also very suitable for IrDA applications are given in table 1.

| Technology | Typical Chip Data | | | | Typical Device | Typical Device Data | | | | |
|--|-----------------------------|-----------------------|---------------------------|----------|----------------|-----------------------------|-----------------------------|------------------|------------------|---|
| | Φ_e/mW at 0.1 A | λ_p/nm | $\Delta\lambda/\text{nm}$ | Polarity | | Φ_e/mW at 0.1 A | Φ_e/mW at 1.5 A | V_F/V at 0.1 A | V_F/V at 1.0 A | $\Phi_e(1.5\text{A})/\Phi_e(0.1\text{A})$ |
| GaAs on GaAs | 7.7 | 950 | 50 | p up | TSUS 540. | 20 | 140 | 1.3 | 2.1 | 9 |
| $\text{Ga}_{1-x}\text{Al}_x\text{As}$ | 6.7 | 875 | 80 | n up | TSHA 550. | 27 | 350 | 1.5 | 3.4 | 13 |
| GaAs + $\text{Ga}_{1-x}\text{Al}_x\text{As}$ on GaAs | 16 | 950 | 50 | p up | TSAL6200 | 35 | 300 | 1.35 | 2.4 | 12 |
| $\text{Ga}_{1-x}\text{Al}_x\text{As}$ on $\text{Ga}_{1-x}\text{Al}_x\text{As}$ | 16 | 870 | 40 | p up | TSHF 5400 | 45 | | 1.5 | | $t_r/t_f/\text{ns}$ 30 |
| $\text{Ga}_{1-x}\text{Al}_x\text{As}$ on $\text{Ga}_{1-x}\text{Al}_x\text{As}$ | 17 | 870 | 40 | p up | TSFF 5410 | 50 | | 1.5 | | $t_r/t_f/\text{ns}$ 15 |

Table 1: Characteristics data of IRED chips

UV, Visible, and Near IR Silicon Photodetectors

(adapted from "Sensors, Vol 6, Optical Sensors, Chapt. 8, VCH – Verlag, Weinheim 1991")

Silicon Photodiodes (PN and PIN Diodes)

The physics of silicon detector diodes

Absorption of radiation is caused by interaction of photons and charge carriers inside a material. Different energy levels allowed and the band structure determine likelihood of interaction and, therefore, absorption characteristics of semiconductors. Long wavelength cutoff of the absorption is given by band-gap energy. The slope of absorption curve depends on physics of interaction and is much weaker for silicon than for most other semiconducting materials. This results in strong wavelength-dependent penetration depth which is shown in figure 8. (The penetration depth is defined as that depth where $1/e$ of the incident radiation is absorbed.)

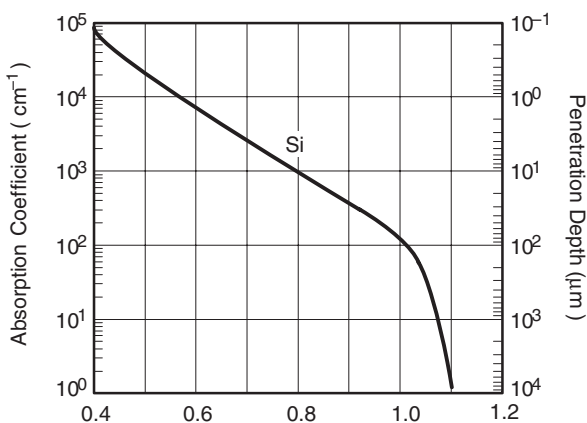


Figure 8. Absorption and penetration depth of optical radiation in silicon

Depending on wavelength, penetration depth varies from tenths of a micron at 400 nm (blue) to more than 100 μm at 1 μm (IR). For detectors to be effective, an interaction length of at least twice penetration depth should be realized (equivalent to $1/e^2 = 86\%$ absorbed radiation). In the pn diode, generated carriers are collected by electrical field of pn junction. Effects in vicinity of a pn junction are shown in figure 9 for various types and operating modes of pn diode. Incident radiation generates mobile minority carriers – electrons in p-side, holes in n-side. In short circuit mode shown in figure 9 (top), carriers drift under the field of the built-in potential of pn junction. Other carriers diffuse inside field-free semiconductor along a

concentration gradient, which results in an electrical current through the applied load, or without load, in an external voltage, open circuit voltage, V_{OC} , at contact terminals. Bending of energy bands near the surface is caused by surface states. An equilibrium is established between generation, recombination of carriers, and current flow through load.

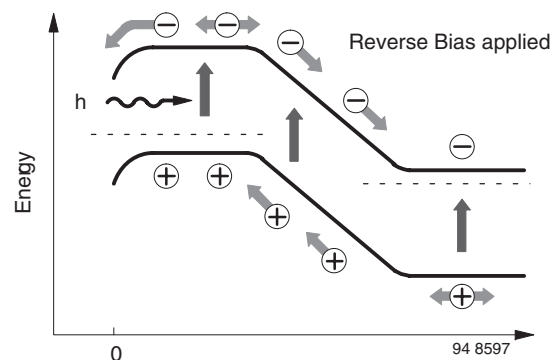
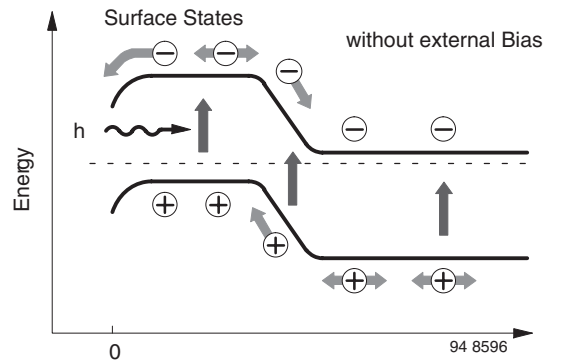


Figure 9. Generation-recombination effects in the vicinity of a pn junction.

Top: Short circuit mode, bottom: reverse biased

Recombination takes place inside bulk material with technology- and process-dependent time constants which are very small near contacts and surfaces of the device. For short wavelengths with very small penetration depths, carrier recombination is the efficiency limiting process. To achieve high efficiencies, as many carriers as possible should be separated by electrical field inside the space charge region. This is a very fast process, much faster than typical recombination times (for data, see chapter 'Operating modes and circuits'). Width, W , of space charge is a function of doping concentration N_B and applied voltage V :

$$W = \sqrt{\frac{2 \times \epsilon_S \times \epsilon_0 \times (V_{bi} + V)}{q \times N_B}} \quad (1)$$

(for a one-sided abrupt junction), where V_{bi} is built-in voltage, ϵ_S dielectric constant of Si, ϵ_0 vacuum dielectric constant and q is electronic charge. The diode's capacitance (which can be speed limiting) is also a function of space charge width and applied voltage. It is given by

$$C = \frac{\epsilon_S \times \epsilon_0 \times A}{W} \quad (2)$$

where A is the area of the diode. An externally applied bias will increase space charge width (see figure 8) with the result that a larger number of carriers are generated inside this zone which can be flushed out very fast with high efficiency under applied field. From equation (1), it is evident that space charge width is a function of doping concentration N_B . Diodes with a so-called pin structure show according to equation (1) a wide space charge width where i stands for intrinsic, low doped. This zone is also sometimes nominated as v or p rather than low doped n , n^- or p , p^- zone indicating the very low doping. Per equation (2), junction capacitance C , is low due to the large space charge region of PIN Photodiodes. These photodiodes are mostly used in applications requiring high speed.

Figure 10, shows cross section of PIN Photodiodes and PN diodes. The space charge width of PIN Photodiodes (bottom) with a doping level ($n = N_B$) as low as $N_B = 5 \times 10^{11} \text{ cm}^{-3}$ is about $80 \text{ } \mu\text{m}$ wide for a 2.5 V bias in comparison with a pn diode with a doping (n) of $N_B = 5 \times 10^{15} \text{ cm}^{-3}$ with only 0.8 mm .

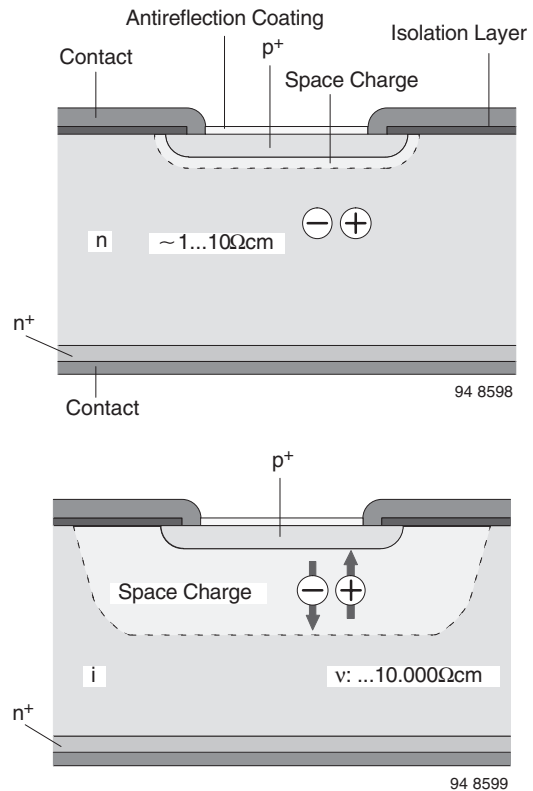


Figure 10. Comparison of PN diode (top) and PIN Photodiode (bottom)

Properties of Silicon Photodiodes

I-V Characteristics of illuminated pn junction

The cross section and I-V-characteristics of a photodiode are shown in figure 11 and 12. Characteristic of the illuminated diode is identical to characteristic of a standard rectifier diode. Relationship between current, I , and voltage, V , is given by

$$I = I_S \times (\exp V/V_T - 1) \quad (3)$$

with $V_T = kT/q$

$k = 1.38 \times 10^{-23} \text{ JK}^{-1}$, Boltzmann constant

$q = 1.6 \times 10^{-19} \text{ As}$, electronic charge.

I_S , the dark-reverse saturation current, is a material and technology-dependent quantity. The value is influenced by doping concentrations at pn junction, by carrier lifetime, and especially by temperature. It shows a strongly exponential temperature dependence and doubles every $8 \text{ } ^\circ\text{C}$.

94 8601

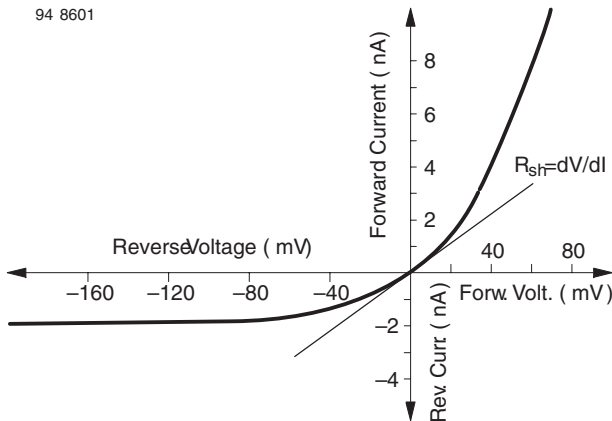


Figure 11. Measured I-V-characteristics of an Si photodiode in the vicinity of the origin

Typical dark currents of Si photodiodes are dependent on size and technology and range from less than picoamps up to tens of nanoamps at room temperature conditions. As noise generators, dark current I_{r0} and the resistance R_{sh} (defined and measured at a voltage of 10 mV forward or reverse, or peak-to-peak) are limiting quantities when detecting very small signals.

The photodiode exposed to optical radiation generates a photocurrent I_r exactly proportional to incident radiant power Φ_e .

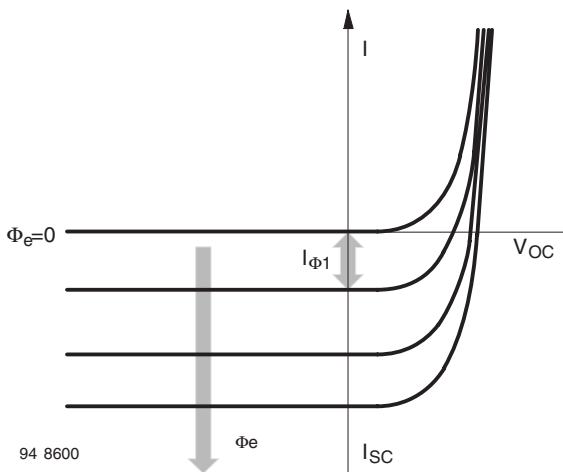


Figure 12. I-V-Characteristics of an Si photodiode under illumination. Parameter: Incident radiant flux.

Quotient of both is spectral responsibility $s(\lambda)$,

$$s(\lambda) = I_r / \Phi_e [A/W] \quad (4)$$

Characteristic of irradiated photodiode is then given by

$$I = I_S \times (\exp V / V_T - 1) - s(\lambda) \times \Phi_e \quad (5)$$

and in case $V \approx 0$, zero or reverse bias we find,

$$I = -I_S - s(\lambda) \times \Phi_e \quad (6)$$

Dependent on load resistance, R_L , and applied bias, different operating modes can be distinguished. An unbiased diode operates in photovoltaic mode. Under short circuit conditions (load $R_L = 0 \Omega$), short circuit current, I_{SC} flows into the load. When R_L increases to infinity, output voltage of the diode rises to open circuit voltage, V_{OC} , given by

$$V_{OC} = V_T \times \ln(s(\lambda) \times \Phi_e / I_S + 1) \quad (7)$$

Because of this logarithmic behavior, open circuit voltage is sometimes used for optical light meters in photographic applications. Open circuit voltage shows a strong temperature dependence with a negative temperature coefficient. The reason for this is exponential temperature coefficient of dark reverse saturation current I_S . For precise light measurement, a temperature control of photodiode is employed. Precise linear optical power measurements require small voltages at the load typically smaller than about 5 % of corresponding open circuit voltage. For less precise measurements, an output voltage half of the open circuit voltage can be allowed. Most important disadvantage of operating in photovoltaic mode is relative large response time. For faster response, it is necessary to implement an additional voltage source reverse biasing the photodiode. This mode of operation is termed photoconductive mode. In this mode, the lowest detectable power is limited by shot noise of dark current, I_S , while in the photovoltaic mode, thermal (Johnson) noise of shunt resistance, R_{sh} , is the limiting quantity.

Spectral responsivity

Efficiency of Si photodiodes:

Spectral responsivity, s_λ , is given as the number of generated charge carriers ($\eta \times N$) per incident photons N of energy $h \times \nu$ (η is percent efficiency, h is Planck's constant, and ν is frequency of radiation). Each photon will generate one charge carrier at the most. Photocurrent I_{re} is then given as

$$I_{re} = \eta \times N \times q \quad (8)$$

$$s_\lambda = I_{re} / \phi_e \quad (9)$$

$$= \eta \times N \times q / (h \times \nu \times N) = \eta \times q / (h \times \nu)$$

$$s_\lambda = \frac{\lambda(\mu m)}{1.24} [A/W]$$

At fixed efficiency, a linear relationship between wavelength and spectral responsivity is valid.

Figure 8 shows that semiconductors absorb radiation similar to a cut-off filter. At wavelengths smaller than cut-off wavelength the incident radiation is absorbed. At larger wavelengths the radiation passes through material without interaction. Cut-off wavelength corresponds to bandgap of material. As long as energy of photon is larger than bandgap, carriers can be generated by absorption of photons, provided that material is thick enough to propagate photon-carrier interaction. Bearing in mind that energy of photons decreases with increasing wavelength, it can be understood, that the curve of the spectral responsivity vs. wavelength in ideal case (100 % efficiency) will have a triangular shape (see figure 13). For silicon photodetectors, cut-off wavelength is near 1100 nm.

In most applications, it is not necessary to detect radiation with wavelengths larger than 1000 nm.

Therefore, designers use a typical chip thickness of 200 μm to 300 μm , which results in reduced sensitivity at wavelengths larger than 950 nm. With a typical chip thickness of 250 μm , an efficiency of about 35 % at 1060 nm is achieved. At shorter wavelengths (blue-near UV, 500 nm to 300 nm) sensitivity is limited by recombination effects near the surface of semiconductor. Reduction in efficiency starts near 500 nm and increases with decreasing wavelength. Standard detectors designed for visible and near IR radiation may have only poor UV/blue sensitivity and poor UV stability. Well designed sensors for wavelengths of 300 to 400 nm can operate with fairly high efficien-

cies. At shorter wavelengths (< 300 nm), efficiency decreases strongly.

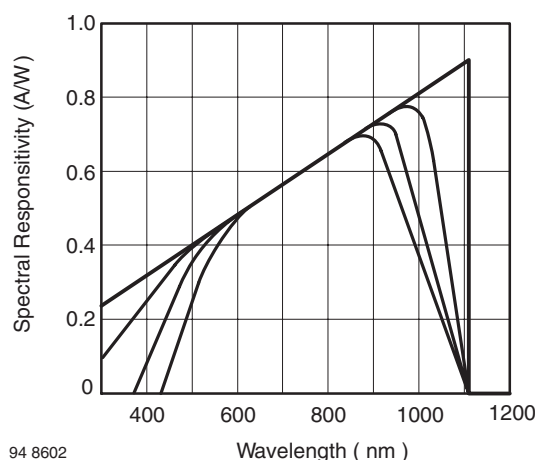


Figure 13. Spectral responsivity as a function of wavelength of a Si photodetector diode, ideal and typical values

Temperature dependence of spectral responsivity

Efficiency of carrier generation by absorption and loss of carriers by recombination are the factors which influence spectral responsivity. Absorption coefficient increases with temperature. Radiation of long wavelength is therefore more efficiently absorbed inside the bulk, and results in increased response. For shorter wavelengths (< 600 nm), reduced efficiency is observed with increasing temperature because of increased recombination rates near the surface. These effects are strongly dependent on technological parameters and therefore cannot be generalized to the behavior at longer wavelengths.

Uniformity of spectral responsivity

Inside technologically defined active area of photodiodes, spectral responsivity shows a variation of sensitivity in the order of < 1 %. Outside defined active area, especially at lateral edges of the chips, local spectral response is sensitive to applied reverse voltage. Additionally, this effect depends on wavelength. Therefore, relation between power (Watt) related spectral responsivity, s_λ (A/W), and power density (Watt/cm²) related spectral responsivity, s_λ [A/(W/cm²)] is not a constant. This relation is a function of wavelength and reverse bias.

Stability of spectral responsivity

Si detectors for wavelengths between 500 nm and 800 nm appear to be stable over very long periods of time. In the literature concerned here, remarks can be found on instabilities of detectors in blue, UV, and

Vishay Semiconductors

near IR under certain conditions. Thermal cycling reversed the degradation effects.

Surface effects and contamination are possible causes but are technologically well controlled.

Angular dependence of responsivity

Angular response of Si photodiodes is given by the optical laws of reflection. Angular response of a detector is shown in figure 14.

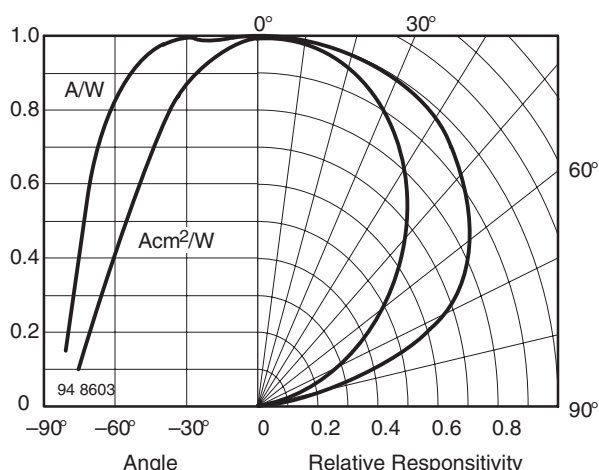


Figure 14. Responsivity of Si photodiodes as a function of the angle of incidence

Semiconductor surfaces are covered with quarter wavelength anti-reflection coatings. Encapsulation is performed with uncoated glass or sapphire windows. Bare silicon response can be altered by optical imaging devices such as lenses. In this way, nearly every arbitrary angular response can be achieved.

Dynamic Properties of Si Photodiodes

Si photodiodes are available in many different variations. Design of diodes can be tailored to meet special needs. Si photodiodes may be designed for maximum efficiency at given wavelengths, for very low leakage currents, or for high speed. Design of a photodiode is nearly always a compromise between various aspects of a specification.

Inside the absorbing material of diode, photons can be absorbed in different regions. For example at the top of a p^+n^- diode there is a highly doped layer of p^+ -Si. Radiation of shorter wavelengths will be effectively absorbed, but for larger wavelengths only a small amount is absorbed. In the vicinity of pn junction, there is the space charge region, where most of the photons should generate carriers. An electric field accelerates the generated carrier in this part of the detector to a high drift velocity. Carriers which are not absorbed in these regions penetrate into field-free

region where the motion of the generated carriers fluctuates by slow diffusion process.

Dynamic response of the detector is composed of different processes which transport carriers to contacts. Dynamic response of photodiodes is influenced by three fundamental effects:

- Drift of carriers in an electric field
- Diffusion of carriers
- Capacitance \times load resistance

Carrier drift in the space charge region occurs rapidly with very small time constants. Typically, transit times in an electric field of $0.6 \text{ V}/\mu\text{m}$ are in the order of $16 \text{ ps}/\mu\text{m}$ and $50 \text{ ps}/\mu\text{m}$ for electrons and holes, respectively. At (maximum) saturation velocity, transit time is in the order of $10 \text{ ps}/\mu\text{m}$ for electrons in p-material. With a $10 \mu\text{m}$ drift region, travelling times of 100 ps can be expected. Response time is a function of distribution of generated carriers and is therefore dependent on wavelength.

Diffusion of carriers is a very slow process. Time constants are in the order of some ms. Typical pulse response of detectors is dominated by these two processes. Obviously, carriers should be absorbed in large space charge regions with high internal electrical fields. This requires material with an adequate low doping level.

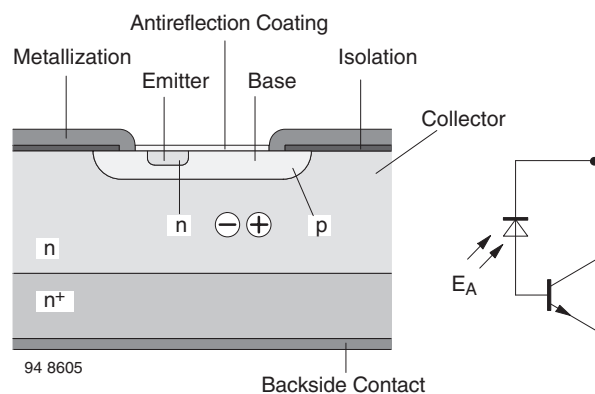
Furthermore, a reverse bias of rather large voltage is useful. Radiation of shorter wavelength is absorbed in smaller penetration depths. At wavelengths shorter than 600 nm , decreasing wavelength leads to an absorption in diffused top layer. Movement of carriers in this region is also diffusion limited. Because of small carrier lifetimes, time constants are not as large as in homogeneous substrate material.

Finally, capacitive loading of output in combination with load resistance limits frequency response.

Properties of Silicon Phototransistors

The phototransistor is equivalent to a photodiode in conjunction with a bipolar transistor amplifier (figure 15). Typically, current amplification, B , is between 100 and 1000 depending on type and application. Active area of phototransistor is usually about $0.5 \times 0.5 \text{ mm}^2$.

Data of spectral responsivity are equivalent to those of photodiodes, but must be multiplied by the factor current amplification, B .



Switching times of phototransistors are dependent on current amplification and load resistance and are between 30 ns and 1 μs. Resulting cut-off frequencies are a few hundred kHz.

The transit times, t_r and t_f , are given by

$$t_{r, f} = \sqrt{\left(\frac{1}{2f_t}\right)^2 + b(RC_B V)^2} \quad (10)$$

f_t : Transit frequency

R : Load resistance

C_B : Base-collector capacitance, $b = 4...5$

V : Amplification

Phototransistors are most frequently applied in transmissive and reflective optical sensors.

Figure 15. Phototransistor, cross section and equivalent circuit